EQUALISATION OF BROADBAND MIMO CHANNELS BY SUBBAND ADAPTIVE IDENTIFICATION AND ANALYTIC INVERSION

Viktor Bale and Stephan Weiss

Communications Research Group, School of Electronics & Computer Science
University of Southampton, Southampton SO17 1BJ, UK
{vb01r,sw1}@ecs.soton.ac.uk

ABSTRACT

This paper introduces the subband method of performing adaptive identification and analytic inversion of broadband MIMO channels. It shows that the techniques can potentially lower the computational cost while improving the performance for highly frequency-selective channel with a long impulse response. It covers subband adaptive identification and shows two methods to invert a broadband MIMO channel, the time-domain and frequency-domain methods. Finally results are shown for adaptation MSE, channel-equaliser MSE and BER performance.

1. INTRODUCTION

Potentially great capacity increases through the use of Multiple-Input Multiple-Output (MIMO) systems have now become well-known. Much of the work in this area has assumed that the sub-channels which comprise the MIMO channels have a flat frequency transfer characteristic. Since one the potential applications of MIMO system is to increase the date rate through the channel to amounts which were not previously possible, it seems far for more realistic that we would use broadband sub-channels which are frequency-selective. To be able to realise the high capacities promised by broadband MIMO channels, we need to develop a high performance low-complexity technique for finding a suitable broadband MIMO equaliser. Further if the equaliser is to be used in a mobile environment we must assume that the channel will temporally dynamic or fading. This further exacerbates the problem of finding and tracking the optimum equaliser so that satisfactory performance is maintained.

A common and simple approach is to use the adaptive NLMS algorithm to adapt to the inverse of the broadband MIMO channel and track it as the channel fades. The problem with this is that the convergence rate of the NLMS algorithm is related to the ratio between the minimum and maximum of the PSD of the input signal to the algorithm [1, 2]. In an adaptive inversion set-up this would be the received signal at the output of the MIMO channel, and since even if they were white at the transmitter they would be coloured by the channel, and hence we would expect slow convergence. In fact it may be so slow that for realistic channels even after several tens or hundreds of thousands of algorithm iteration the adaptation mean squared error (MSE) still may not reach an acceptably low value [3]. In addition to this the computational cost involved in performing such a long adaptation can quickly become unacceptably high for large MIMO channels with long impulse responses. A further potential problem is that for fading mobile channels even if the equaliser is calculated beforehand using an analytic method, the adaptive inversion may not be able to track the equaliser at a fast enough rate and it may soon become useless. Using a fast converging algorithm such as the RLS also has associated problems as the complexity is greater than the NLMS and hence for large broadband MIMO system the cost may be unacceptable. Further the RLS may exhibit worse performance than LMS-type algorithms when tracking dynamic system [4].

A promising solution proposed in [3] was to employ subband adaptive techniques to invert the channel. The convergence rate was shown to be greater and the computational cost lower than the fullband method. Hence the subband inversion may be better able to track a dynamic equaliser at a lower cost. In order to use this method for tracking though, we must first initialise the equaliser to the optimum at a point in time. Although subband adaptive inversion showed improved convergence over the fullband approach, it is still too slow to use this method to initialise the equaliser in the first instance. Hence we must use an alternative method which is the subject of this paper. We propose to use a subband adaptive identification of the broadband MIMO channel, which can be performed using many fewer iterations than the inversion, followed by a computationally efficient analytic inversion. The whole process must also be performed in subbands as the subband adaptive tracking system must be initialised with the subband equaliser coefficients. The system consider is shown in Figure 1.

Sec. 2 briefly introduces the technique of subband processing, while Sec. 3 covers subband adaptive identification and explains the potential computational cost advantage. Sec. 4 develops the time-domain and frequency-domain methods of inverting the subband representation of a MIMO system, states the costs of the inversions and also explains some associated problems and methods to overcome them. Finally, in Sec. 5 simulations results are presented before discussing conclusions in Sec. 6.

2. SUBBAND TECHNIQUE

2.1. Oversampled Subband Decomposition

In essence the subband approach involves the partitioning of the input signals into a finite number, K, of frequency bands or subbands. This is similar to transforming the problem into the frequency domain and is performed in practice by a class of band-pass filters, but unlike this the signals remain as time-domain sequences. Since the subband signals are now bandlimited by a factor K more than the fullband signals, we may downsample each of the signals by a factor $N \leq K$. Fig. 2 shows a simple subband system, which filters input signal $u[n]$ through an analysis filter bank comprising K band-pass filters $a_k[n], k = 0, 1, \cdots, K-1$, decimates the signals by N, upsamples by N and reconstructs the original fullband signal by passing through synthesis filters $s_k[n]$ and summing. Any signal processing task can be performed on the decimated subband signals [2].

2.2. Modulated Filter Banks

The filters banks are often created using a generalised discrete Fourier transform (GDFT) [5], which have the advantage that all the band-pass filters can be created by modulating a common prototype filter to the correct frequency. Secondly they have the desirable property that the synthesis filter bank is simply the parahermitian of the analysis banks when the system is expressed using a polyphase representation [2].

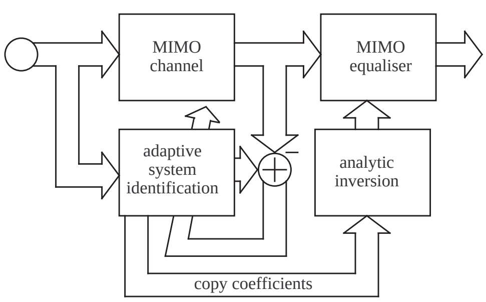

Fig. 1. System setup with adaptive MIMO system identification and analytic inversion to calculate the MIMO equaliser.

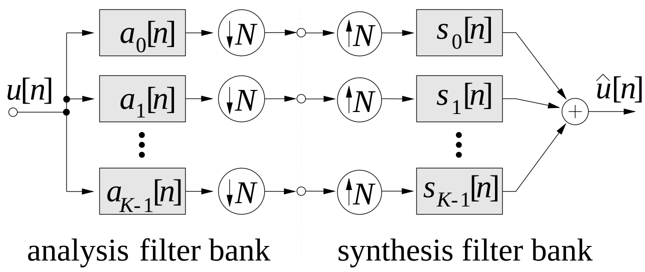

Fig. 2. Subband decomposition by mean of analysis and synthesis filtering banks.

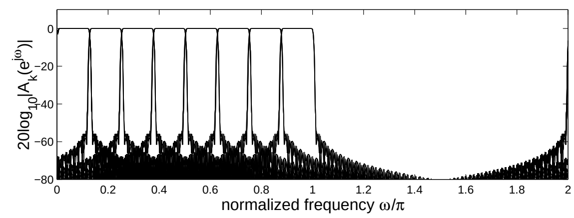

Fig. 3. Filter bank characteristic for K = 16 and N = 14 based on a prototype filter with $L_p = 448$ coefficients.

2.3. Complexity

Although $K = N$ would result in the greatest computational savings when performing an adaptive algorithm, spectral aliasing limits the performance of any processing in the subband domain and in practice we oversample the signals whereby we choose N slightly less than K [6]. An example of an analysis filter bank where $K = 16$ and $N = 14$ is shown in Fig. 3, where magnitude responses $A_k(e^{j\omega}) \bullet\!\!-\!\!\circ\; a_k[n]$ of only the first 8 filters are shown. The computational cost involved in the analysis and synthesis filtering process is [7]

$$C_{\text{bank}} = (2L_p + 4K \log_2 K + 8K)/N, \tag{1}$$

per fullband sample period, where L_p is the prototype filter length.

3. ADAPTIVE IDENTIFICATION

3.1. Multi-Channel Filtering

The first step involved in finding the optimum equaliser in subbands is to adaptive identify a $M \times P$ MIMO channel. We use a multi-channel form of the NLMS algorithm, whereby the adaptive filter state vectors of each channel are stacked, which effectively transforms the problem into a single-channel form. The M inputs transmitted through the MIMO channel excite P signals at the receivers, which can be expressed as

$$\mathbf{y}[n] = \mathbf{H}\mathbf{x}[n] + \boldsymbol{\nu}[n], \tag{2}$$

where $\mathbf{x}[n] \in \mathbb{C}^{ML_h}$ contains M stacked input signal vectors of equal to the channel length L_h

$$\mathbf{x}[n] = [\mathbf{x}_1^T[n] \quad \mathbf{x}_2^T[n] \quad \cdots \quad \mathbf{x}_M^T[n]]^T \tag{3}$$

and $\mathbf{x}_m[n] = [x_m[n] \quad x_m[n-1] \quad \cdots \quad x_m[n-L_h+1]]^T, \quad p = 1(1)M$. The noise vector $\boldsymbol{\nu}[n] \in \mathbb{C}^P$ contains P noise samples taken from a white Gaussian source

$$\boldsymbol{\nu}[n] = [\nu_1[n] \quad \nu_2[n] \quad \cdots \quad \nu_P[n]]^T. \tag{4}$$

The received signal vector at time n, $\mathbf{y}[n]$, is length P and defined analogously to (4). Finally, the channel is defined

$$\mathbf{H} = \begin{bmatrix} \mathbf{h}_{11}^T & \mathbf{h}_{21}^T & \cdots & \mathbf{h}_{M1}^T \\ \mathbf{h}_{12}^T & \mathbf{h}_{22}^T & \cdots & \mathbf{h}_{M2}^T \\ \vdots & \vdots & \ddots & \vdots \\ \mathbf{h}_{1P}^T & \mathbf{h}_{2P}^T & \cdots & \mathbf{h}_{MP}^T \end{bmatrix} \tag{5}$$

where $\mathbf{h}_{mp} = [h_{mp}[0] \quad h_{mp}[1] \quad \cdots \quad h_{mp}[L_h-1]]^T$ is the channel impulse response between the m^{th} transmitter and p^{th} receiver. Notice that for the purpose of channel identification we assume that the channel is static.

3.2. Optimum Subband Identification

Next we derive the subband adaptive system which will adapt to the unknown $\mathbf{H}$, using the received samples $y_p[n],\ p = 1(1)P$ as the desired signals and a known training sequence as the input signals $x_m[n],\ m = 1(1)M$. Fig. 4 shows one of P multiple-input single-output (MISO) adaptive blocks that run in parallel and are required to identify the MIMO channel. Each MISO system adapts in subbands to the M sub-channels between the transmitters and a particular receiver.

The outputs of the subband adaptive units within the MISO system for receiver p are given by

$$\hat{y}_{p,k}[n] = \hat{\mathbf{h}}_{p,k}^T[n]\mathbf{x}_k[n], \quad k = 1(1)K,\ p = 1(1)P, \tag{6}$$

where $\hat{\mathbf{h}}_{p,k}[n] = [\hat{\mathbf{h}}_{1p,k}^T[n] \quad \hat{\mathbf{h}}_{2p,k}^T[n] \quad \cdots \quad \hat{\mathbf{h}}_{Mp,k}^T[n]]^T$ and $\hat{\mathbf{h}}_{mp,k}[n] = [\hat{h}_{mp,k}[0,n] \quad \hat{h}_{mp,k}[1,n] \quad \ldots \quad \hat{h}_{mp,k}[L_{h,s}-1),n]]^T$ is the impulse response of the adaptive filter which models the sub-channel between the m^{th} transmitter and p^{th} receiver in the k^{th} subband and depends on time n due to the fact that the system is adaptive, and $L_{h,s}$ is the length of the subband adaptive filter. There is some freedom in choosing in $L_{h,s}$ and the value depends on factors such as the size of L_h relative to L_p, but a value in the range $L_{h,s} = [L_h/N, (L_h + 2L_p)/N]$ is usually chosen. Further in (6) $\mathbf{x}_k[n] = [\mathbf{x}_{1,k}[n] \quad \mathbf{x}_{2,k}[n] \quad \cdots \quad \mathbf{x}_{M,k}[n]]^T$, where $\mathbf{x}_{m,k}[n]$ is the subband filter state vector at time n corresponding to $x_{m,k}$. We may now define K subband error signals for the p^{th} receiver

$$e_{p,k}[n] = y_{p,k}[n] - \hat{y}_{p,k}[n] \quad k = 1(1)K,\ p = 1(1)P. \tag{7}$$

Following the usual Weiner-Hopf type analysis [1] for each subband we arrive at the optimum adaptive filter solution

$$\hat{\mathbf{h}}_{p,k,\mathrm{opt}} = \mathbf{R}_{xx,k}^{-1}\mathbf{p}_{p,k}, \tag{8}$$

where $\mathbf{R}_{xx,k}$ is the auto-correlation matrix of the filter state vector in the k^{th} subband $\mathbf{x}_k[n]$, and $\mathbf{p}_{p,k}$ is the cross-correlation vector between the subband filter state vector and desired signal $y_{p,k}[n]$. Hence the update step of the subband multichannel NLMS algorithm follows as

$$\hat{\mathbf{h}}_{p,k}[n+1] = \hat{\mathbf{h}}_{p,k}[n] + \tilde{\mu}\frac{\mathbf{x}_k[n]e_{p,k}^*[n]}{\mathbf{x}_k^H[n]\mathbf{x}_k[n]} \tag{9}$$

where $\tilde{\mu}$ is the normalised adaptation step-size coefficient.

3.3. Identification Complexity

The computational cost of the fullband NLMS algorithm is

$$C_{\mathrm{FB}} = P(8ML_h + 8M + 10). \tag{10}$$

One of the main advantages of the subband approach is a reduction in computational cost. Not only are the adaptive filters generally shorter but the adaptive update can executed at $1/N^{th}$ of the rate of the fullband version due to the decimation. Of course the algorithm must be performed K times in parallel, once for each subband. The cost of the subband NLMS algorithm hence accrues to

$$C_{\mathrm{SB}} = \frac{PK}{N}(8ML_{h,s} + 8M + 10) + \frac{M+P}{N}C_{\mathrm{bank}} \tag{11}$$

per fullband sampling period. To be able perform a direct comparison between the fullband and subband cost, we must decide on a relationship between L_h and $L_{h,s}$. An often quoted relationship is $L_{h,s} = (L_h + L_p)/N$, which would result in

$$\begin{aligned} C_{\mathrm{SB}} &= \frac{PK}{N}(8M(L_h + L_p)/N + 8M + 10) \\ &\quad + \frac{M+P}{N}C_{\mathrm{bank}}. \end{aligned} \tag{12}$$

per fullband sampling period. However the simulations presented later use a value for $L_{h,s}$ closer to L_h/N. The analysis filtering operation causes a fixed computational overhead, and for small $L_h \ll L_p$ we may find that the subband adaptation is actually more costly than the fullband version. Hence the subband method is generally more suitable for high bandwidth channels with a long impulse response.

4. ANALYTIC INVERSION

The second part of the task is to analytically invert the subband-identified MIMO channel. We are constraining the equaliser

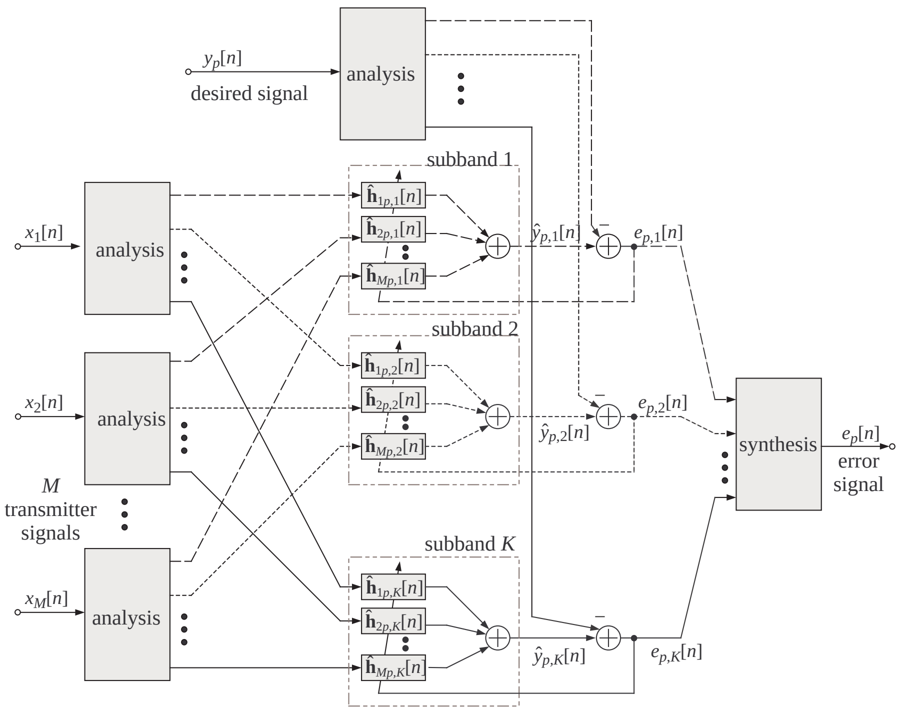

Fig. 4. A MISO subband adaptive system arranged for system identification.

to be a linear FIR system, and there are two methods we use to invert the channel. These two methods have been demonstrated for fullband channel inversion in [8], but we shall briefly review them and apply the subband technique here.

4.1. Time-Domain Inversion

The time-domain inversion technique, so-called as it arranges the time-dispersiveness of the broadband MIMO channel a two dimensional matrix, calls for the creation of convolutional matrices. Each sub-channel has its own convolutional matrix and these are augmented and stacked to create a larger "parent" MIMO convolutional matrix [8,9].

The convolutional channel matrix between m^{th} transmitter and p^{th} receiver for the k^{th} subband is given by

$$\bar{\mathbf{H}}_{mp,k} = \begin{bmatrix} \mathbf{h}_{mp,k}^H & \cdots & \cdots & 0 & 0 \\ 0 & \mathbf{h}_{mp,k}^H & \cdots & \ddots & 0 \\ 0 & 0 & \ddots & \ddots & \vdots \\ 0 & 0 & \cdots & \mathbf{h}_{mp,k}^H & \cdots \end{bmatrix}. \quad (13)$$

We may construct a parent convolutional matrix $\mathbf{H}$ over all m and p for subband k, yielding

$$\bar{\mathbf{H}}_k = \begin{bmatrix} \bar{\mathbf{H}}_{11,k} & \bar{\mathbf{H}}_{21,k} & \cdots & \bar{\mathbf{H}}_{M1,k} \\ \bar{\mathbf{H}}_{12,k} & \bar{\mathbf{H}}_{22,k} & \cdots & \bar{\mathbf{H}}_{M2,k} \\ \vdots & \vdots & \ddots & \vdots \\ \mathbf{H}_{1P,k} & \mathbf{H}_{2P,k} & \cdots & \mathbf{H}_{MP,k} \end{bmatrix}, \quad (14)$$

where $\bar{\mathbf{H}}_k$ is of dimensions $PL_{g,s} \times M(L_{h,s} + L_{g,s} - 1)$ and $L_{g,s}$ is the subband MISO equaliser length for each sub-channel. From this we may develop an expression for the optimum solution for the $M \cdot P$ equaliser filters for the k^{th} subband

$$\mathbf{g}_{m,k} = (\bar{\mathbf{H}}_k \bar{\mathbf{H}}_k^H + \frac{\sigma_\nu^2}{\sigma_x^2}\mathbf{I})^\dagger \bar{\mathbf{H}}_k \mathbf{d}_m, \quad (15)$$

where $\mathbf{d}_m$ is a channel selection and delay vector and $\{\cdot\}^\dagger$ refers to the pseudo-inverse [10] which is required for valid cases where $M > P$ but $\bar{\mathbf{H}}_k \bar{\mathbf{H}}_k^H$ may be rank-deficient. This calculation must be performed for all $m = 1(1)M$ and $k = 1(1)K$ to create a K MIMO equalisers, one for each subband. These can then be placed between analysis and synthesis filter banks to create the full equaliser system.

The computational complexity of the subband time-domain method is $\mathcal{O}(L_g^3)$. Since the subband filters are potentially up to N times shorter than the fullband equalisers it is evident that the cost of inverting a single subband is $\mathcal{O}(N^3)$ lower, but this must be performed K times, hence the computational saving afforded by the subband technique is $\mathcal{O}(N^3/K)$.

Although this method will result in an optimum subband solution the cost of the inversions, even though much less than the fullband method, can still grow rapidly with increasing $L_{g,s}$ to unacceptable levels. Since we are dealing with high bandwidth channels this is likely to be a problem.

4.2. Frequency-Domain Inversion

A solution to the problem of the computational cost growing rapidly for the time-domain inversion is to use lower complexity method, and frequency-domain inversion is a good candidate to this end. We may transform the impulse response of each of sub-channel for each subband into its bandlimited spectral representation using a length $L_{g,s}$ FFT, and hence formulate the problem in the frequency-domain. For each subband we now have $L_{g,s}$ scalar valued $M \times P$ matrices, one for each frequency-bin of the FFT, which can easily be inverted using a standard matrix inversion algorithm. Hence the zero-forcing inverse for each frequency bin in each subband is given by the pseudo-inverse of that channel, i.e.

$$\mathbf{G}_k[f] = e^{-j2\pi d}(\mathbf{H}_k^H[f]\mathbf{H}_k[h])^{-1}\mathbf{H}_k^H[f]. \qquad (16)$$

Unfortunately the matter is complicated by a phenomenon that affects frequency-domain multiplications known as circular convolution, or the wrap-around effect [11]. In essence a convolution in the frequency-domain differs from the true linear convolution when performed in time-domain at either end of the resultant signal or system, and the shorter the FFT the worse the problem becomes. A solution is to use a regularisation factor in the inversion, giving a new definition for the inverse [12]

$$\mathbf{G}_k[f] = e^{-j2\pi d}(\mathbf{H}_k^H[f]\mathbf{H}_k[h] + \beta\mathbf{I})^{-1}\mathbf{H}_k^H[f] \qquad (17)$$

where β is the regularisation factor. The method of regularisation is a powerful technique for finding the solutions of ill-posed problems. Also it can be shown that if $\beta = \sigma_\nu^2/\sigma_x^2$, i.e. the noise-to-signal ratio (NSR) then at low SNR values the system MSE performance approaches that of the optimum time-domain method [13]. At some critical SNR, the MSE performance will start to degrade as the NSR falls below a value that results in the best performance possible using the subband frequency-domain method in a noiseless environment. At this critical SNR we would gain a better performance result by switching to a fixed regularisation factor.

One pertinent difference between the subband and fullband frequency-domain inversion is due to the relative lengths of the equaliser. Since the subband adaptive filters are generally shorter than the channel impulse response length, we may often also use shorter subband equaliser filters than would have been necessary for the fullband system. Unfortunately a shorter equaliser will worsen the wrap-around effect and may degrade the performance of the subband system more than we would have otherwise expected. By how much the performance is worsened will be shown in the simulations.

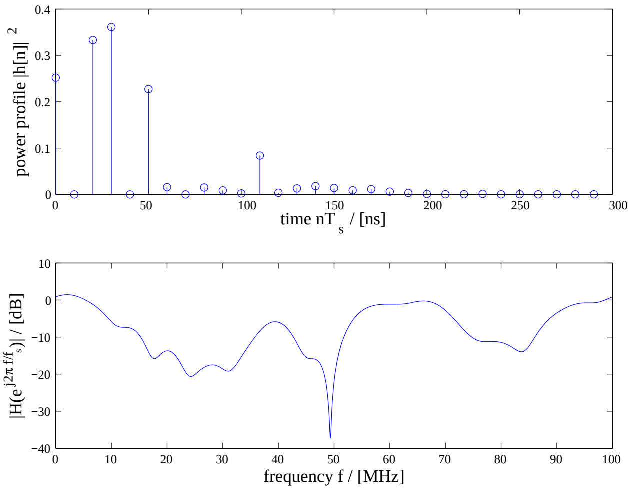

Fig. 5. CIR sampled at 100 MHz (top) and magnitude response (bottom) of a sample channel generated by the SV model.

The main motivating factor for the use of the frequency-domain inversion method is that is requires less computational power than the time-domain method. It can be shown that the FFTs are the computationally dominant part of the inversion process and hence the complexity is $\mathcal{O}(L_{g,s}\log_2 L_{g,s})$. Evidently the savings offered by the subband approach are now much smaller than for the time-domain inversion method. In fact, we shall see in the simulations that it is possible that for short equalisers where $L_g \ll L_p$ the savings may not outweigh the analysis and synthesis filtering cost overhead.

5. SIMULATION RESULTS

5.1. MIMO Channel Model and Simulation Parameters

We use the Saleh-Valenzuela statistical indoor model to generate realistic channel impulse responses (CIRs) [14]. The SV model produces a clusters of rays according to an exponential distribution. Following the suggestions in [14], we have simulated two sets of CIRs at sampling rates of 100MHz and 1GHz with a mean cluster arrival time $1/\Lambda = 300$ ns, a mean ray arrival time $1/\lambda = 5$ ns, a cluster power decay time constant $\Gamma = 60$ ns and the ray power decay time constant $\gamma = 20$ ns [14]. The magnitude response of a typical SV channel, band-limited and sampled at 100 MHz, is shown in Fig. 5. We generate four of these channels independently to create a 2×2 broadband MIMO channel. Simulations are then run on an ensemble of such 2×2 MIMO channel realisations.

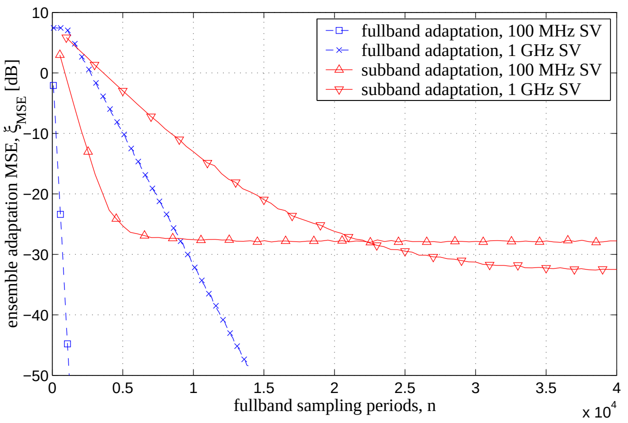

Fig. 6. MIMO channel identification adaptation MSE for fullband and subband adaptations with 100 MHz and 1 GHz-sampled SV channel.

For the analytic inversions, we have selected a delay $d = L_{g,s}/2$ to address the non-minimum phase characteristic of the channel. For the NLMS adaptations we use $\tilde{\mu} = 0.18$. For the fullband processing and the 100 MHz-sampled SV channel we use $L_h = 30$ and $L_{g,f} = 280$, where $L_{g,f}$ is the fullband equaliser length, and for the 1 GHz-sampled SV channel we use $L_h = 300$ and $L_{g,f} = 980$. For the equivalent subband system we use $K = 16$, $N = 14$ based on a prototype filter with $L_p = 448$ taps resulting in the characteristic given in Fig. 3 and have set $L_{h,s} = 12 > L_{h,f}/N$ and $L_{g,s} = 29 > L_{g,f}/N$ for the 100 MHz-sampled SV channel, and $L_{h,s} = 44 > L_{h,f}/N$ and $L_{g,s} = 70 = L_{g,f}/N$ for the 1 GHz-sampled SV channel.

5.2. Adaptive Identification

The fullband and subband adaptive identification MSE behaviour for a 2×2 100 MHz and 1 GHz-sampled channels is shown in Figure 6. As expected the fullband techniques show the quickest convergence because $L_{g,s} > L_{h,s}/N$ and also as the input signals are white the subband method will not demonstrate an convergence improvement.

The real power of the subband system in this case arises from the reduction in computational cost. Table 1 shows the cost per fullband sampling period in multiply-accumulate computations (MACs) of the subband and fullband adaptive identification of the 100 MHz and 1 GHz-sampled 2×2 SV channels. We see the for the 100 MHz-sampled channel the subband adaptation requires about 84% of the computations needed for the fullband technique. For the 1 GHz-sampled channel, this becomes 21%. Hence we see that the relative savings offered by the subband method increase as the channel impulse response, and hence equaliser length increases.

This is a fair comparison assuming that the adaptations

adaptation, channel	cost (MACs)
subband, 100 MHz SV	846
fullband, 100 MHz SV	1,012
subband, 1 GHz	2,034
fullband, 1 GHz SV	9,652

Table 1. Computational cost (MACs) per fullband sampling period of fullband and subband adaptive identification for the 100 MHz and 1 GHz-sampled 2×2 MIMO channels.

inversion, channel	cost (MACs)
TD Sub, 100 MHz SV	3.9×10^5
FD Sub, 100 MHz SV	2.25×10^3
TD Full, 100 MHz	2.2×10^7
FD Full, 100 MHz SV	2.28×10^3
TD Sub, 1 GHz SV	5.49×10^6
FD Sub, 1 GHz SV	6.86×10^3
TD Full, 1 GHz SV	9.41×10^8
FD Full, 1 GHz SV	9.74×10^3

Table 2. Evaluation of the computational cost of various combinations of time-domain (TD) and frequency-domain (FD), and subband and fullband inversion, for the 100 MHz and 1 GHz-sampled SV channel.

are a continuous process, but as we simply need to reach a specified MSE and the fullband method converges much quicker, we find that the total operation count may in fact be greater for the subband technique. For example, for the 100 MHz channel, -20 dB MSE is reached in 14% of the time it takes the fullband method, and hence the overall computation count for the fullband is 16.8% of that for the subband. For the 1 GHz-sampled channel though this ratio becomes about 245%, meaning that for this long channel the subband adaptation has lower cost in all respects.

5.3. Analytic Inversion

The system MSE after using the various analytic inversion methods discussed in this paper is shown in Figure 7. The system MSE refers to the error between the input to the MIMO channel and the channel-equaliser response to this input. The method labelled "Full" corresponds to fullband inversion of a known channel and the time-domain inversion (TD Full) represents the optimum performance possible from any of the systems. The curves labelled "SuS" refers to subband identification followed by subband inversion, where as "SuF" represent subband identification after which the equivalent fullband system is found by passing a impulse through the analysis filter bank, the subband filters and the synthesis filter bank, and finally this is inverted in the fullband. Also shown are curves for frequency-domain inversion regularised by the NSR (FDN) and also by a heuristically optimised fixed value which results in the best possible performance in a noiseless environment (FDO). We have no result for the fullband inversion of the known channel for the 1 GHz-sampled SV channel as the channel is of such length that it would be computationally unfeasible, however we have included SuF results for this channel for interest. We see that generally at lower SNR value the FDN curves approach the optimum performance of the TD curves, and that as the SNR rises the FDN curves begin to worsen due to circular convolution but the FDO curves continue to improve until the best achievable MSE is reached.

The cost of performing these inversions is shown in Table 2, where the complexity orders are evaluated. For the time-domain inversion significant savings are offered by the subband method as expected. However for the frequency-domain inversion the savings are much lower and evidently for these simulations only just compensate for the analysis filtering overhead (the synthesis filter bank is not required for the purposes of identifying the channel).

Comparing the computational costs of the inversion process which is performed only once with the cost of the subband identifications in Table 1 which must be performed for many thousands of iterations it is evident that the identification will dominate the overall computational cost.

5.4. BER Performance

Figure 8 show the BPSK BER performance for the various systems developed in this paper. The systems are the same as those in Figure 7, but the simulations are now performed only over a "realistic" SNR range of 0 dB to 30 dB. We see that for the 100 MHz-sampled SV channel the performances are all quite similar. Only the FDO curves are worse as the point where a fixed regularisation factor outperforms the noise power value occurs at about 30 dB. The performance of the 1 GHz-sampled SV channel is the best due to the much longer equaliser filters.

6. DISCUSSION

In this paper we have introduced a method of adaptively identifying a broadband MIMO channel and analytically inverting to create an MIMO equaliser in subbands. The performance results and computational costs indicate that for channels with a short impulse response, or for channels that are not particularly frequency-selective the subband approach is of limited use. However, for much longer channels, such as the 300 coefficient 1 GHz-sampled SV channel, the advantages offered by technique are much more impressive. Not only does subband processing lower the computational cost involved in identifying and inverting the channel, but also the BER performance is quite satisfactory. Finally, this method of finding a subband equaliser for broadband MIMO channels is useful for initialising an adaptive equaliser for dynamically fading channels where we would use subband-adaptive inversion to track the equaliser. Subband-adaptive inversion has shown the ability to converge faster from coloured input signals and hence may be able to facilitate superior tracking performance than the equivalent fullband system [3].

7. REFERENCES

[1] S. Haykin, *Adaptive Filter Theory*, Prentice Hall, Englewood Cliffs, 3rd edition, 1996.

[2] S. Weiss and R. W. Stewart, *On Adaptive Filtering in Oversampled Subbands*, Shaker Verlag, Aachen, Germany, 1998.

[3] V. Bale and S. Weiss, "A Low-Complexity Subband Adaptive MIMO Equaliser for Highly Frequency-Selective Channels," in *Spectral Methods and Multi-rate Signal Processing*, Vienna, Austria, September 2004, pp. 61–68.

[4] N.J Bershad and O.M. Macchi, "Adaptive Recovery of a Chirped Sinusoid in Noise, Part 1: Performance of the RLS Algorithm," *IEEE Transactions on Signal Processing*, vol. 39, no. 3, pp. 583–594, March 1991.

[5] P. P. Vaidyanathan, *Multirate Systems and Filter Banks*, Prentice Hall, Englewood Cliffs, 1993.

[6] A. Gilloire and M. Vetterli, "Adaptive Filtering in Subbands with Critical Sampling: Analysis, Experiments and Applications to Acoustic Echo Cancelation," *IEEE Transactions on Signal Processing*, vol. SP-40, no. 8, pp. 1862–1875, August 1992.

[7] S. Weiss, "Analysis and Fast Implementation of Oversampled Modulated Filter Banks," in *Mathematics in Signal Processing V*, J. G. McWhirter and I. K. Proudler, Eds., chapter 23, pp. 263–274. Oxford University Press, March 2002.

[8] V. Bale and S. Weiss, "Comparison of Analytic Inversion Techniques for Equalisation of Highly Frequency-Selective MIMO Systems," in *Proceedings of Workshop on Signal Processing for Wireless Communications*, King College, London, UK, June 2004, pp. 150–155.

[9] O. Kirkeby, P. A. Nelson, F. Orduna-Bustamante, and H. Hamada, "Local Sound Field Reproduction Using Digital Signal Processing," *Journal of the Acoustical Society of America*, vol. Vol.100, no. No.3, pp. 1584–1593, March 1996.

[10] G. Strang, *Linear Algebra and Its Applications*, Academic Press, New York, 2nd edition, 1980.

[11] J. J. Shynk, "Frequency-Domain and Multirate Adaptive Filtering," *IEEE Signal Processing Magazine*, vol. 9, no. 1, pp. 14–37, January 1992.

[12] O. Kirkeby, P. A. Nelson, H. Hamada, and F. Orduna-Bustamante, "Fast Deconvolution of Multichannel Systems Using Regularization," *IEEE Transactions on Speech and Audio Processing*, vol. 6, no. 2, pp. 189–194, March 1998.

[13] V. Bale, *Computationally Efficient Equalisation of Broadband Multiple-Input Multiple-Output Systems*, Mini-Thesis, University of Southampton, UK, 2004.

[14] A. A. M. Saleh and R. A. Valenzuela, "A Statistical Model for Indoor Multipath Propagation," *IEEE Journal on Selected Areas of Communications*, vol. 5, no. 2, pp. 128–137, February 1987.

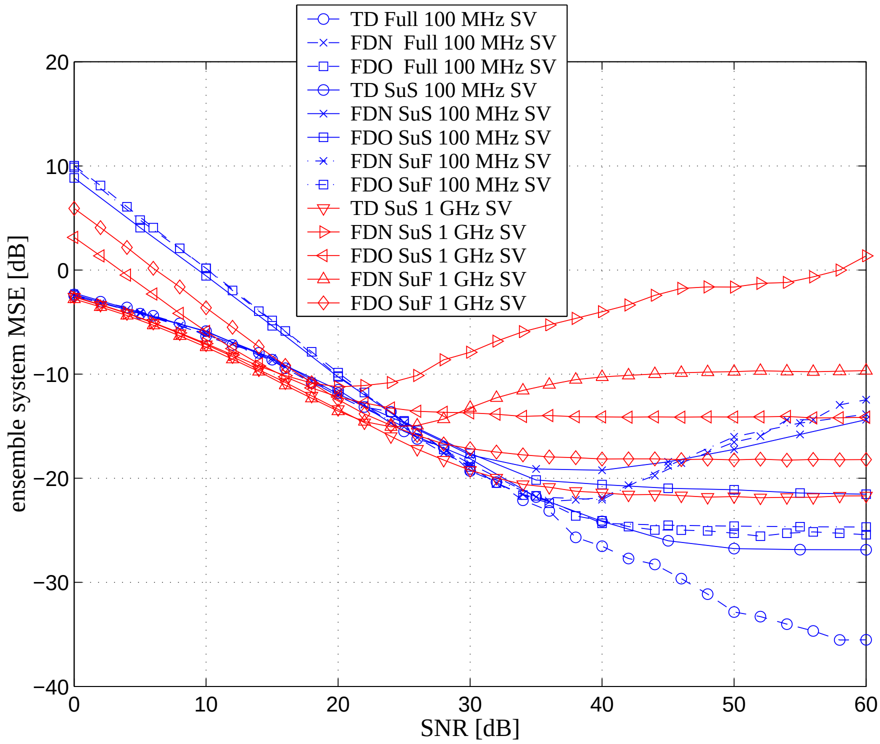

Fig. 7. System MSE versus SNR behaviour for subband and fullband analytic inversion for a 100 MHz and 1 GHz-sampled SV channel.

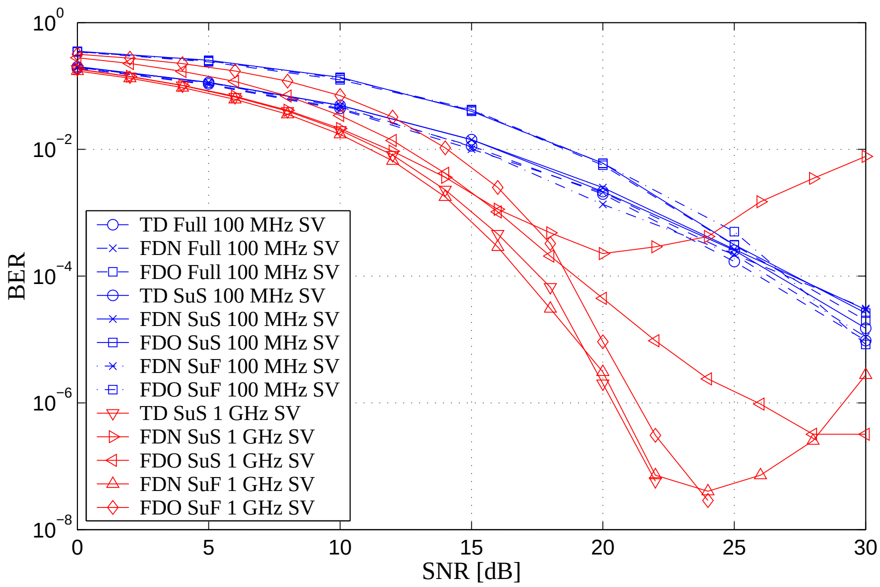

Fig. 8. BER versus SNR performance for subband and fullband equalisers for a 100 MHz and 1 GHz-sampled SV channel.